Environmental Science Processes & Impacts

ROYAL SOCIETY OF CHEMISTRY

COMMUNICATION

View Article Online
View Journal | View Issue

Cite this: *Environ. Sci.: Processes Impacts*, 2025, **27**, 892

Received 10th December 2024
Accepted 7th March 2025

DOI: 10.1039/d4em00766b

rsc.li/espi

Effects of urban particulate matter on the secondary structure of albumin†

Samal Kaumbekova,[a] Naoya Sakaguchi,[b] Yuto Miyamoto,[b] Atsuto Onoda,[c] Yasuhiro Ishihara[d] and Masakazu Umezawa *[ab]

Particulate air pollution is an environmental problem recognized as a global public health issue. Although the toxicological effects of environmental particle matter (PM) have been reported, the mechanism underlying the effect of PM on protein conformational changes, which are associated with the development of various diseases, has yet to be elucidated. In this study, we investigated the effect of urban PM on the secondary structure of proteins using bovine serum albumin (BSA). An urban aerosol (CRM28) was used as the original PM (PMO) and washed with acetone to investigate the effect of PM with two different chemical compositions. After washing with acetone, the remaining PM fraction contained decreased amounts of ions and carbon, while the metallic concentration was increased; thus, this PM fraction was labeled as PMM. After incubation of BSA with PM, the samples were subjected to Fourier-transform infrared (FT-IR) spectroscopy to investigate the changes in the absorption peak of the amide I band. BSA incubated with PMO and PMM showed an increase in the β-sheet ratio to the total secondary structure. Furthermore, the β-sheet content was more significantly increased when mixed with PMM (by 22.6%), indicating a more significant effect of the metallic fraction on the formation of β-sheets. In comparison, the lowest total amount of α-helix and β-sheets (with a decrease of 8.5%) was observed after incubation with PMO, associated with the protein partial unfolding in the presence of ions and carbonaceous PM constituents. The potential of a long-term effect of PM composition on protein structure would be of future interest in *in vivo* time-course studies.

Environmental significance

Air pollution, represented by atmospheric particulate matter (PM), is an environmental problem recognized as a global public health issue. While protein structural stability is important for its proper functionality, the changes in the protein secondary structure are associated with the development of various diseases, including Alzheimer's Disease (AD). Although the toxicological effects of PM on living organisms and the progression of various diseases were revealed in previous studies, the mechanisms underlying the effect of PM on protein conformational changes remain unclear. In this study, we investigated the changes in the secondary structure of albumin protein after incubation with PM fractions with different compositions, highlighting the significance and toxicological effects of various PM constituents, such as metals, ions, and carbons.

Introduction

Particulate air pollution exposure over the entire lives of individuals is an environmental disaster taking place all over the world.[1,2] Smaller particles in the particulate matter (PM), known as fine particulate matter ($PM_{2.5}$) with an aerodynamic diameter of equal or less than 2.5 μm, majorly produced from industrial emissions, biomass burning, domestic heating, and tobacco smoking, lead to more severe adverse effects on living qualities than larger particles.[3] In particular, $PM_{2.5}$ is known to affect the respiratory tract, penetrate deep into the lungs, enter the bloodstream, and impact cardio- and cerebrovascular systems and other organs.[4] This problem is a major health concern for both developing and developed countries. Over the past 30 years, extensive evidence has shown that air pollution affects cardiovascular and respiratory morbidity and mortality across the world.[5] While the annual average range of $PM_{2.5}$ differs from 10 to 100 μg m^{-3} globally,[6] the World Health Organization (WHO) also declares that "it is unacceptable to still have 7 million preventable deaths and countless preventable lost years of good health due to air pollution",[4] including $PM_{2.5}$.

In more recent years, evidence has been accumulating from human epidemiological and animal studies, suggesting that air pollution may negatively affect brain function and contribute to

[a]*Department of Medical and Robotic Engineering Design, Faculty of Advanced Engineering, Tokyo University of Science, 6-3-1 Niijuku, Katsushika, Tokyo 125-8585, Japan. E-mail: masa-ume@rs.tus.ac.jp*

[b]*Department of Materials Science and Technology, Faculty of Advanced Engineering, Tokyo University of Science, 6-3-1 Niijuku, Katsushika, Tokyo 125-8585, Japan*

[c]*Department of Hygienic Chemistry, Faculty of Pharmaceutical Sciences, Sanyo-Onoda City University, 1-1-1 Daigaku-dori, Sanyo-Onoda City, Yamaguchi 756-0884, Japan*

[d]*Program of Biomedical Science, Graduate School of Integrated Sciences for Life, Hiroshima University, 1-7-1, Kagamiyama, Higashi-Hiroshima, Hiroshima 739-8521, Japan*

† Electronic supplementary information (ESI) available. See DOI: https://doi.org/10.1039/d4em00766b

adverse neurological outcomes, although the interaction mechanisms are difficult to elucidate due to the enormous complexity of the nervous system and nature of air pollution.[7,8] Inhaled $PM_{2.5}$ reaches the brain by pathways through the nasal epithelial layer and the lungs,[9,10] suggested by evidence of the presence of metal particles in human brains.[11] Therefore, the brain is one of the targets of $PM_{2.5}$. With 57 million people worldwide suffering from dementia in 2019, this number is estimated to increase to 153 million by 2050;[12] thus, the neurotoxicity of environmental factors such as $PM_{2.5}$ on brain functions has been a priority research topic.

Numerous experimental studies have also indicated that PM plays an important role in AD development and progress; however, some scientific gaps remain in the complete picture of PM-induced AD toxicity. In particular, limited studies examined the real effects underlying the environmental level of $PM_{2.5}$ exposure. For example, subchronic exposure to environmental levels of $PM_{2.5}$ increases oxidative stress that leads to neuronal dysfunction in AD transgene mice.[13] An association between particulate air pollution and cognitive decline through activation of systemic inflammatory pathways and vascular dysfunction has been reported.[7] Minimum doses of pollution can be handled by the organism when this exposure is acute, but the same doses administered chronically lead to excess oxidative stress that can produce neurodegeneration.[7] White matter hyperintensities (WMH) linked to cognitive deficiencies, with increased concentrations of inflammatory markers and decreased total brain volume, were observed in children and young adults exposed to air pollution in Mexico City.[14] Epidemiological studies have shown associations of PM exposure with decreased brain volume, a marker of age-associated brain atrophy.[15] Particularly, atmospheric $PM_{2.5}$ concentration positively correlates with AD onset[16] and with the number of hospitalizations due to AD.[17] In addition, $PM_{2.5}$ concentration also correlates with the observation of amyloid deposition in biological tissues,[13] suggesting an effect of $PM_{2.5}$ on AD pathology.

While the typical PM constituents are organic carbon (OC), elemental carbon (EC), metals, and secondary inorganic water-soluble ions, the PM composition might vary depending on the major sources of emission, location, and seasonal variations.[18] Our previous studies also demonstrated that maternal exposure to low doses of carbon black (CB) nanoparticles (NPs), engineered NPs used as a particulate air pollution model, induces brain perivascular inflammation in offspring mice.[19–21] In particular, mice offspring experienced a chronic intense state of environmental stress and exhibited an early brain imbalance of neural communication following maternal exposure to CB-NPs[21] and diesel exhaust particles.[22] Moreover, alteration in the cerebral gene expression was observed from the fetal exposure to metal oxide NPs, associated with the changes in the olfactory bulb and cerebral cortex of mice offspring.[23] Furthermore, recent studies have also correlated the chronic impact of polycyclic aromatic hydrocarbons (PAHs), a typical constituent of motor-vehicle exhaust and tobacco smoke, which are often adsorbed on ambient PM, with the progression of neurodegenerative disorders. While $PM_{2.5}$ exposure induces chronic inflammation in the brain, including the olfactory bulb and cerebral cortex, PAHs adsorbed on the PM surface likely contribute to this inflammatory effect.[24] Chronic inflammation, a major mechanism of AD, can be caused by oxidative stress[25] which is also related to cognitive dysfunction in AD model mice.[26]

Previous studies have also shown the potential effects of PM and PM constituents on the alterations of protein conformation, including the induced formation of β-sheet structures associated with the progression of various diseases, such as AD.[27] For example, the perivascular accumulation of proteins with β-sheet structures was observed in the brain of mice offspring due to maternal exposure to CB-NPs.[19] Moreover, previous molecular dynamics (MD) studies showed accelerated formation of amyloid β (Aβ) peptide oligomers with altered secondary structure in the presence of carbonaceous ultrafine PM models with various surface modifications[28] and water-soluble ions.[29] Furthermore, recent MD studies suggest that PAHs strongly interact with Aβ peptides, the principal component of the amyloid plaques found in the brains of people with AD, *via* hydrophobic and hydrogen-bond-based forces resulting in secondary structure changes, including β-sheet increase.[30,31] In addition, in our recent *in vitro* studies, metal NPs induced changes in the protein structure, promoting the loss of α-helices and the formation of β-sheets either in the presence of co-existing ions[32,33] or due to the surface functionalization of NPs by amine groups.[34] Moreover, PAHs present with metal ions in tobacco smoke also affected the aggregation process of Aβ peptides in a recent *in vitro* study,[35] indicating the importance of the synergistic effect of carbonaceous and metallic content of PM.

While previous studies showed the toxicological effect of PM, experimental studies on the impact of PM constituents on the protein secondary structure are limited. In this study, by using BSA as a model of proteins abundant in body fluids such as blood and cerebrospinal fluid,[36,37] we aimed to investigate the mechanism by which PM components accelerate changes in the protein structure. Moreover, while 90% of Aβ peptides in human blood are bound to albumin, albumin inhibits the formation of amyloid fibrils.[38,39] Consequently, the additional indirect impact of PM on the progression of AD was studied[39] by examining the effect of PM fractions with different compositions on the albumin conformation. In particular, two types of PM compositions were studied: an originally collected urban PM sample from the air in Beijing (PMO) before washing with acetone and a PM sample obtained after washing with acetone. Furthermore, considering that after washing with acetone, the PM sample contained more metals, the sample was labeled as PMM. While the simple mixtures used in this study are not physiologically relevant, the molecular mode of action can be observed in our experiments. Infrared absorption spectra of the samples incubated with BSA were analyzed by Fourier-transform infrared (FT-IR) spectroscopy to observe the absorption peak of the amide I band (1600–1700 cm^{-1}) that is affected by secondary structure changes of BSA.[40,41] Overall, BSA incubated with PM showed a statistically significant increase in the β-sheet ratio to the total secondary structure. Moreover, at low PM concentrations, the increase in the β-sheet ratio was larger when mixed with PMM than the case with PMO, suggesting enhanced toxicity of the metallic portion of PM.

Materials and methods

Materials

BSA and deuterium oxide (D_2O) were purchased from Sigma-Aldrich Co. (St Louis, MO, USA) and were used without further purification.

PM composition

Urban aerosols collected from filters in a central ventilation system in a building in the Beijing City Center from 1996 to 2005 (CRM28) were purchased from the National Institute for Environmental Studies. CRM28 was sieved using a 32 μm sieve. The diameters of over 40% of CRM28 particles were less than two μm, and 99% of the particles were less than 10 μm in the original urban PM (PMO) fraction. The adsorbed chemicals on CRM28 were removed by washing as described previously,[42] a simplified flowchart summarizing the experimental workflow is shown in Fig. 1. Briefly, distilled water was added to CRM28 (PMO fraction), and then the mixture was centrifuged to remove water-soluble chemicals. This procedure was repeated with acetone and dichloromethane (DCM). The resulting pellets were used as PMM fraction. Water-soluble ions were measured by ion chromatography, metal and sulfur contents were determined by using inductively coupled plasma-mass spectrometry, carbons were examined by thermal-optical method, and PAH concentration was determined by GC-MS (7890A/5957C, Agilent, Palo Alto, CA, USA) as was described previously.[24] The full chemical compositions of PMM and PMO fractions are shown in Table S1,† with the simplified chemical composition illustrated in Table 1. While slightly enhanced concentrations of Mg, Al, Fe, and Ti metals were obtained in the PM sample by acetone washing of PMO, 89% of PAHs were removed in the washed PM (Table 1). In the following, due to the high content of metals, the washed PM sample is abbreviated as PMM.

Table 1 Chemical compositions (μg g^{-1}) of PM[a]

	PMM	PMO
Soluble ions		
NO_3^-	6961	18 040
SO_4^{2-}	46 711	81 304
Ca^{2+}	24 506	40 732
Metals and sulfur		
Mg	15 800	14 000
Al	72 000	50 400
K	17 100	13 700
Ca	54 200	66 900
Ti	3690	2920
Fe	40 200	29 200
S	14 800	39 100
Carbons		
Organic carbon	23 505	57 369
Elemental carbon	17 758	64 709
PAHs[b]		
Total PAHs	3.1	27

[a] The full chemical compositions of the PM samples before washing (PMO) and after washing with acetone (PMM) are shown in Table S1. [b] PAHs = polycyclic aromatic hydrocarbons.

Fourier transform infrared spectroscopy for albumin mixed with PM

FT-IR spectroscopy, which is sensitive to protein structural changes,[40,41] was used to elucidate the effect of PM on the BSA conformation. Five distinct conditions were studied, such as BSA in no PM, 0.3 mg mL^{-1} PMM, 3 mg mL^{-1} PMM, 0.3 mg mL^{-1} PMO, and 3 mg mL^{-1} PMO. BSA (30 mg mL^{-1}) and PM samples were mixed in D_2O and incubated for 24 h at room temperature. 20 μL of the sample under the study was dropped onto the sample stage and sandwiched with a spacer (thickness: 0.025 mm) between two CaF_2 plate windows using an Omni-Cell kit (Specac Ltd., Orpington, UK). Fourier transform-infrared spectroscopy (FT-IR) was performed using an FT/IR-6200 spectrometer (JASCO Co., Tokyo, Japan). One hundred scans were averaged for each FT-IR spectrum to account for within-group variation, and three measurements were taken for each condition to account for between-group variation. Similar to previous studies,[32,41] herein, D_2O was used as the solvent instead of H_2O water to avoid overlapping of the bending mode of H–O–H at around 1600 cm^{-1} with the amide I peak of proteins. Gaussian fitting was performed on the infrared absorption spectrum

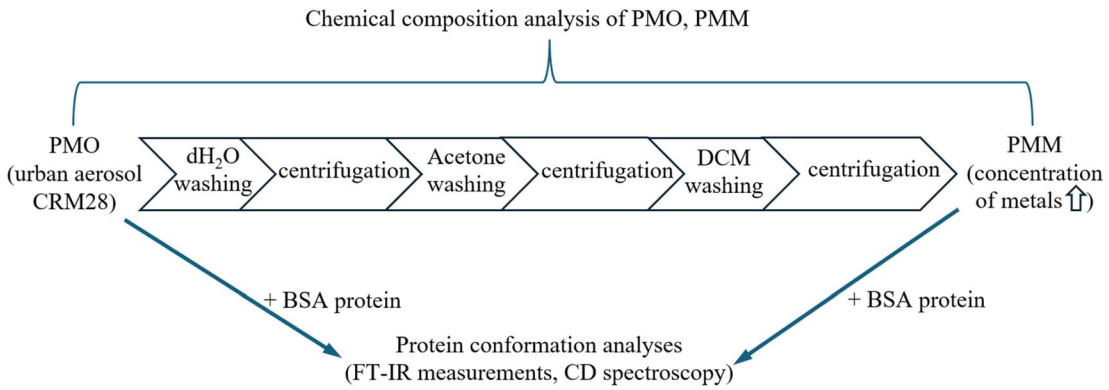

Fig. 1 A flowchart summarizing the experimental workflow.

measured for BSA protein by fixing the position of the absorption peak and varying the height and width of each structural component, such as α-helix (1647 cm^{-1}) and β-sheet (1625 cm^{-1}).[40,43] Considering the α-helix and β-sheet structures as particularly dominant in Amide I absorption, the corresponding ratios to the entire Amide I (1700–1600 cm^{-1}) were represented to characterize the protein structural changes in the presence of PM samples.

Statistical analysis

The statistical significance of the observed protein structural changes was assessed using the Real Statistics Analysis Tool add-in for Excel. The analysis was based on three FT-IR measurements performed under five distinct conditions, including BSA in the absence and presence of PM (0.3 mg mL^{-1} and 3 mg mL^{-1}). First, the Shapiro–Wilk and Levene's tests were used to assess the normality and homogeneity of variance, respectively, for the measured percentage compositions of α-helix and β-sheet in the five samples. Since the data for both α-helix and β-sheet compositions were normally distributed with homogeneous variances, a one-way ANOVA was applied to determine whether there were statistically significant differences in protein secondary structure composition among the five samples. Following a significant ANOVA result, a post-hoc Tukey HSD (Honestly Significant Difference)/Kramer test was conducted to identify specific statistical differences in α-helix and β-sheet compositions between the control sample (no PM) and each of the other four samples individually. A *p*-value threshold of 0.05 was used to determine statistical significance. The results of the statistical analyses are provided in the ESI (Excel file).†

Results

The full chemical compositions of the PM samples before washing (PMO) and after washing with acetone (PMM) are shown in Table S1,† and the simplified composition is shown in Table 1. The PM constituents were classified into several groups, such as soluble ions (Cl^-, NO_3^-, SO_4^{2-}, Na^+, NH_4^+, K^+, Mg^{2+}, and Ca^{2+}), metals (Mg, Al, K, Ca, Ti, Fe, Zn) and sulfur, carbons (OC and EC), and PAHs (fluoranthene, chrysene, benzo[*b*]fluoranthene, benzo[*k*]fluoranthene, benzo[*e*]pyrene, benzo[*a*]pyrene, indeno[1,2,3-*cd*]pyrene, dibenz[*a*,*h*]anthracene, benzo[*ghi*]perylene, and coronene). According to Table 1, among different PM constituents, the PMO sample mainly contained high concentrations of ions (81 304 μg g^{-1} SO_4^{2-}, 40 732 μg g^{-1} Ca^{2+}, 18 040 NO_3^-), metals (66 900 μg g^{-1} Ca, 50 400 μg g^{-1} Al, and 39 100 μg g^{-1} S), carbons (64 709 μg g^{-1} EC and 57 369 μg g^{-1} OC), and PAHs (27 μg g^{-1}). Considering the carbonaceous fraction of PMO, the carbon (EC and OC) contributed to 24.6% of the total mass of PMO, in agreement with the previous study, where the carbonaceous components (EC and OC) contributed to 25.3% of $PM_{2.5}$ concentration measured in Beijing in 2017–2018, associated with fossil fuel combustion.[44] Similarly, the concentration of SO_4^{2-} is high (contributing to 16.4% of the total PMO mass), consistent with the previous study,[44] where the highest concentration of sulfates (18.7%) was observed in the summer in Beijing in 2017–2018, associated with high conversion of SO_2 to SO_4^{2-} at high temperature and relative humidity. Our results were also consistent with a previous source apportionment model, which characterized the metallic composition of $PM_{2.5}$ in Beijing during 2018–2019, revealing high mass concentrations of Ca (586.98 ng m^{-3}) and Al (378.03 ng m^{-3}).[45]

In comparison, after washing the PM fraction with acetone, the remaining PMM sample contained significantly reduced amounts of ions (46 711 μg g^{-1} SO_4^{2-} and 24 506 μg g^{-1} Ca^{2+}), carbons (17 758 μg g^{-1} EC and 23 505 μg g^{-1} OC), and PAHs (3.1 μg g^{-1}), with slightly increased concentrations of most of the metals, such as Mg (15 800 μg g^{-1}), Al (72 000 μg g^{-1}), K (17 100 μg g^{-1}), Ti (3690 μg g^{-1}), and Fe (40200 μg g^{-1}). The results were associated with the washing out of a major portion of the water-soluble ions, and hydrophobic carbons adsorbed on CRM28.

The effect of PMO and PMM samples on the BSA secondary structure after incubation for 24 h was further investigated *via* FT-IR spectroscopy, which is sensitive to protein conformational changes occurring upon functional transitions or intermolecular interactions.[40,41] In addition, the effect of two concentrations of PM samples (0.3 mg mL^{-1} and 3 mg mL^{-1}) was analyzed. The representative FT-IR plots for each sample are shown in Fig. 2, and the corresponding replicates are shown in Fig. S1.† Taking into account two major components of the amide I region, such as α-helix and β-sheets (with a corresponding peak at 1647 cm^{-1} and 1625 cm^{-1} on FT-IR plots, respectively[40,43]), the percentage ratio of α-helix and β-sheets to BSA's total amide I spectra were quantified (Fig. 3). According to Fig. 3, on average, the addition of 0.3 mg mL^{-1} of PMM and PMO suppressed the α-helix percentage ratio from 86.67% to 80.42% and 78.04%, while increasing the β-sheets composition ratio from 8.09% to 9.91% and 8.73%, respectively. Similarly, at higher PM concentrations of 3 mg mL^{-1}, both PMM and PMO suppressed the α-helix percentage ratio to the values of 78.96% and 79.90%, simultaneously increasing the β-sheets ratio to 9.30% and 8.82%, respectively. The statistically significant difference in the changes of the protein secondary structure composition in the presence of PM was verified by statistical analyses, such as ANOVA: single factor and Tukey test, with a *p*-value of less than 0.05 (ESI†).

While both PMM and PMO decreased α-helical content, there was no significant correlation with the PM composition and concentration. Interestingly, the increase in the β-sheet ratio was larger in the presence of PMM compared with PMO at both concentrations under the study, with a more prominent effect at a low concentration of PMM, suggesting that the metallic content of PM might contribute more significantly to the formation of β-sheets in protein structure. Furthermore, the sum of both α-helix and β-sheets ratios to the amide I region was comparatively lower in the presence of PM, indicating the enhanced formation of more unstructured motifs. A more significant decrease was observed in the presence of 0.3 mg mL^{-1} PMO, where the total α-helix and β-sheets composition decreased to 86.77% from 94.76% (in the absence of PM),

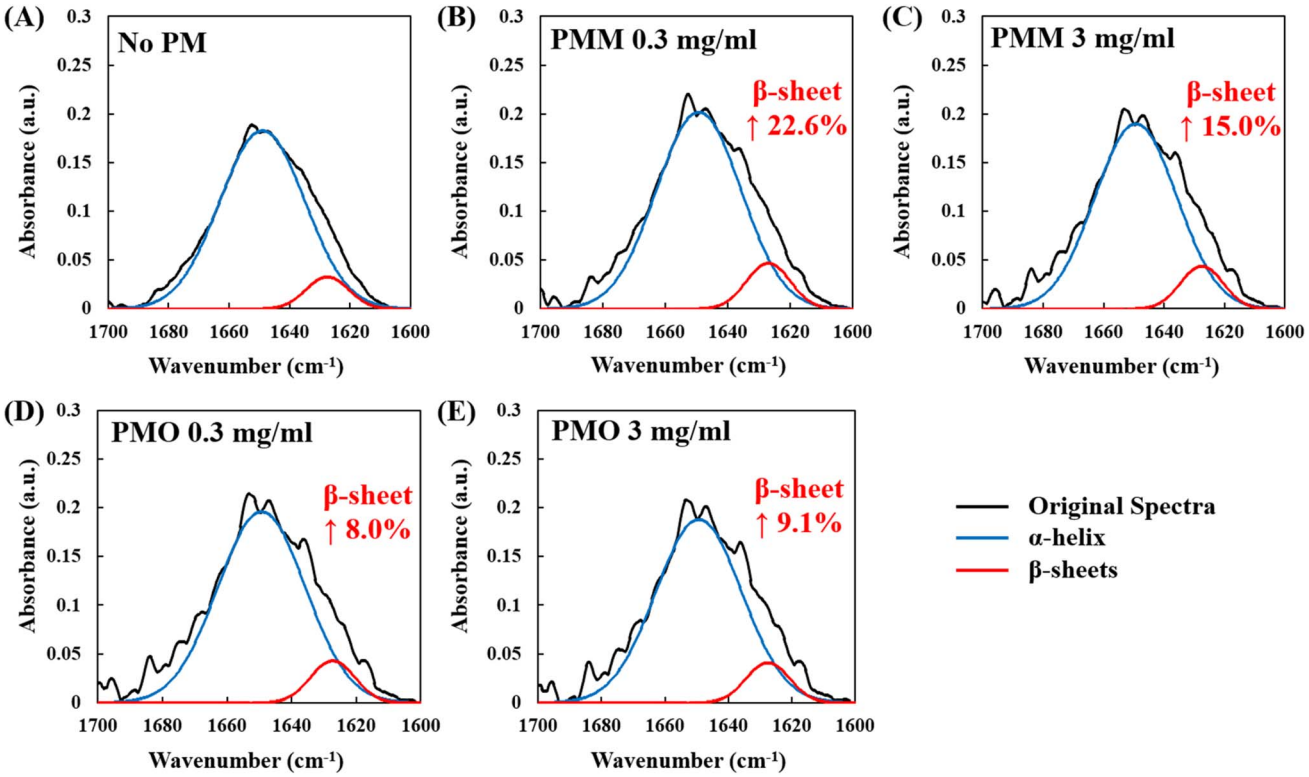

Fig. 2 Amide I absorption spectra of BSA (30 mg mL^{-1}) stirred for 24 h with different PM compositions and concentrations: (A) no PM, (B) 0.3 mg mL^{-1} PMM, (C) 3 mg mL^{-1} PMM, (D) 0.3 mg mL^{-1} PMO, and (E) 3 mg mL^{-1} PMO. In the presence of PM, the FT-IR analysis showed suppressed amounts of α-helix and elevated amounts of β-sheets. The percentage increase in β-sheets relative to the "no PM" condition is shown for each corresponding sample with PM.

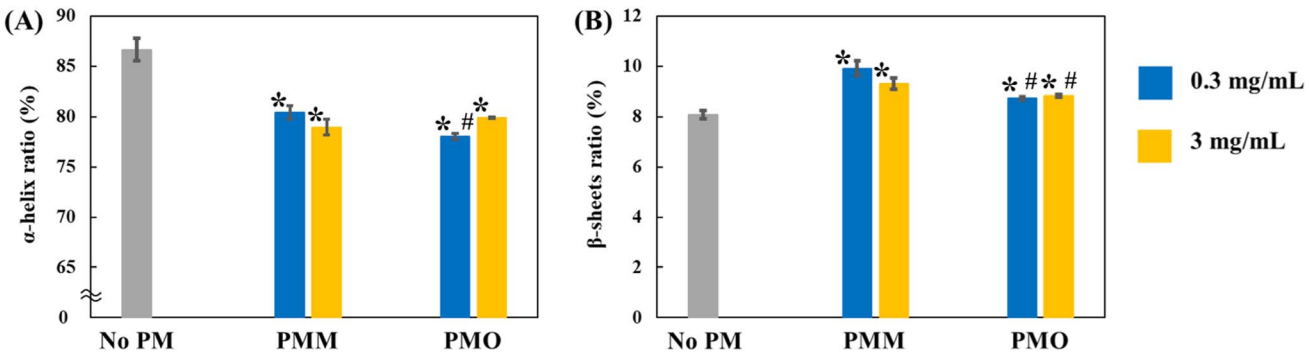

Fig. 3 The percentage ratio of (A) α-helix and (B) β-sheets of the total amide I spectra of BSA stirred for 24 h with different PM compositions and concentrations (*$p < 0.05$ *vs.* "no PM", #$p < 0.05$ *vs.* the "PMM 0.3 mg mL^{-1}" sample).

indicating the enhanced formation of more unstructured motifs in PMO at low PM concentrations.

Discussion

Oligomeric peptides and proteins form self-assembly organizations, such as β-sheet and α-helical conformations, *via* the synergistic effect of non-covalent interactions. In the past two decades, the self-assembly mechanisms of peptides associated with different neurodegenerative diseases, including AD, PD, and Huntington's disease, have been studied,[46,47] mainly focusing on understanding the mechanisms of β-sheet formation.[48] In particular, the loss of helical structures in Aβ peptides and the formation of β-sheets were associated with the growth of amyloid fibrils, associated with the progression of AD.[49] Controlling self-assembly of proteins to form nanostructures is also an essential means for the synthesis of functional nanomaterials in biomedical fields,[50] because the nanostructure of proteins is closely associated with their *in vivo* function, degradation, and clearance. Protein conformation and self-assembly of peptides can be controlled by various factors,

such as changing pH,[51] ion concentrations,[32] and solvent polarity.[52] Furthermore, the twist of peptide chains and hydration environment changes can lead to the early formation of aggregation-prone conformations in the self-assembly of peptides.[53]

Herein, the results of our study showed structural changes in the BSA protein after incubation for 24 h with PM samples with two various compositions containing different concentrations of water-soluble ions, metals, carbonaceous particles, and PAHs. In particular, FT-IR spectra analysis showed the loss of α-helix content and the formation of β-sheets in albumin after incubation with PM with two different compositions. Furthermore, a more prominent effect on the formation of β-sheets was observed in the presence of 0.3 mg mL^{-1} of PMM fraction with high metallic content (72 000 μg g^{-1} of Al, 54 200 μg g^{-1} of Ca, and 40 200 μg g^{-1} of Fe in PM) at decreased concentrations of the ionic and carbonaceous PM constituents. Although the PMM fraction also contained ions (such as 46 711 μg g^{-1} of SO_4^{2-}) and carbonaceous content (23 505 μg g^{-1} of OC and 17 758 μg g^{-1} of EC), their concentrations were significantly decreased in PMM in comparison to the PMO composition, suggesting their minor co-existing contribution towards the induced formation of β-sheets. Furthermore, considering that the total percentage ratio of α-helix and β-sheets to the total amide I spectra of BSA was decreased from 94.76% to 86.77% in the presence of 0.3 mg mL^{-1} of PMO, this observation might be correlated with the enhanced formation of additional unstructured motifs (such as coils and turns) in the presence of ions and carbonaceous content.

Although in our study, BSA was used as a protein model with high helical content and low propensity to form protein aggregates at physiological conditions,[36] early studies reported promoted aggregation of Aβ peptides in the presence of Al(III), in comparison to Zn(II) and Cu(II).[54] Similarly, an *in vitro* study showed spontaneous aggregation of α-synuclein protein involving the formation of β-pleated sheet by incubation with iron.[55] Moreover, enhanced formation of β-sheet/-turn structures was observed in bone morphogenetic protein 2 (BMP-2) in the presence of Ca^{2+}.[56] The previous study also highlighted the induced precipitation of β-sheets of Aβ peptides in senile plaque cores by the synergistic co-existing effect of Al(III) and Fe(II)/Fe(III), explaining the oxidative damage associated with the β-sheets formation *in vivo*.[57] Interestingly, a counteracting mechanism of metals and PAHs present in cigarette smoke on the aggregation kinetics of Aβ peptides was revealed by *in vitro* study,[35] indicating the importance of the synergistic effect of metals and carbonaceous PM constituents.

Considering the mechanism of the formation of β-sheets in the presence of fine and ultrafine particles, adsorption of BSA on the PM surface may locally contrate BSA and result in the formation of hydrogen bonding between aggregated proteins to increase β-sheet structure.[29,58] Such intramolecular interaction could be reduced by soluble ions on PM, possibly owing to stronger interaction *via* electrostatic force between the ions and BSA, as shown by less increase in β-sheet of BSA by PMO with a high content of water-soluble ions. Furthermore, taking into the simultaneous loss of both ordered secondary structure motifs, α-helix, and β-sheets, in the presence of PMO, this observation might be associated with the protein partial unfolding on the surface of PM with high amounts of carbonaceous content, consistent with our previous modeling studies.[28]

Considering the complex composition of PM, the results of our *in vitro* study bring new insights into the facilitating effects of insoluble metallic PM constituents on the formation of β-sheets in the protein structure. While both soluble and insoluble fractions of PM might bring cytotoxicity,[59,60] recent *in vivo* studies showed toxicological effects of water-insoluble components of PM, associated with the changes in the metabolism in mice[61] and locomotion behavior in animal model *C. elegans*.[62] Moreover, the possible translocation mechanism of the water-insoluble components of $PM_{2.5}$ was shown *via* olfactory sensory neurons used as an *in vitro* model.[63]

Reactions as studied *in vitro* in this study may happen *in vivo* if PM, even a trace amount, reaches the brain. The potential translocation of fine and ultrafine particles from the lung to other organs, including the brain, was previously reported by *in vivo* studies.[9] Furthermore, a high content of Al was measured in the human brain tissues of donors with familial AD (up to 33.48 μg g^{-1} dry wt. in the occipital lobe of the brain) taken from the brain bank of the Universidad de Antioquia, Medellin, Colombia.[64] In addition, the passage of exogenous fine particles from the lung into the brain in animals and humans was recently reported, highlighting the retention of inhaled particles (such as isotope-labeled CB) in the mice brain for a longer time in comparison to other organs.[10] Likewise, the possibility that environmental carbonaceous air pollutants can reach the brain and remain in the brain for long periods has been reported by previous *in vivo* studies.[65,66] Furthermore, although there may also be a contribution of metallic elements, it has already been reported *in vivo* that carbonaceous nanoparticles increase protein β-sheet structure in the brain.[67]

Although albumin, a transport protein with high abundancy in blood and high helical content, was used as a protein model in this *in vitro* study, our results showed the induced changes in the protein structure in the presence of two different PM compositions. Considering the limitation of our study, *in vivo* studies focusing on the long-term effect of PM composition on protein structure, including Aβ peptides, would require a time-course study, which would take a large amount of time and will be performed in future works.

Conclusion

Protein structural changes and the formation of β-sheets are important in the context of the progression of various diseases, including AD. While the toxicological effect of PM was previously reported by numerous studies, in this study, the effect of PM on the protein conformation was investigated *in vitro*. Overall, the changes in BSA secondary structure by PM were observed in the amide I band of its FT-IR spectra. Moreover, the increase in the β-sheet ratio was larger after incubation with the PMM fraction with high concentrations of metals in comparison to the PMO fraction, suggesting that the metallic

components of PM might contribute more significantly to the β-sheet increase in albumin. Although the PMM fraction contained ions and carbonaceous content, their concentrations were notably decreased in comparison to the PMO composition, suggesting their minor co-existing contribution towards the induced protein conformation. Nevertheless, *in vivo* studies focusing on protein structural changes and aggregation due to long-term PM exposure would require a time-course study, which will be performed in future works.

Data availability

Data for this article, including the results of the Fourier Transform Infrared Spectroscopy (FT-IR) analyses, are available at **https://tus.box.com/s/smuifs32gfx8zj6k3nqvwhlfqhowlulv**.

Conflicts of interest

There are no conflicts to declare.

Acknowledgements

This work was in part supported by the Japanese Society for the Promotion of Science (JSPS) KAKENHI (Grant Number: 22H03335 and 23K18403), Japan Science and Technology Agency (JST) FOREST Program (Grant Number: JPMJFR225B), the Environment Research and Technology Development Funds of the Environmental Restoration and Conservation Agency of Japan (JPMEERF20205007 and JPMEERF20245004), the Smoking Research Foundation (2024G032) and Kato Memorial Bioscience Foundation.

References

1 J. Lelieveld, J. S. Evans, M. Fnais, D. Giannadaki and A. Pozzer, The contribution of outdoor air pollution sources to premature mortality on a global scale, *Nature*, 2015, **525**(7569), 367–371.
2 P. Biswas, S. A. Polash, D. Dey, M. A. Kaium, A. R. Mahmud, F. Yasmin, *et al.*, Advanced implications of nanotechnology in disease control and environmental perspectives, *Biomed. Pharmacother.*, 2023, **158**, 114172.
3 A. Mukherjee and M. Agrawal, A global perspective of fine particulate matter pollution and its health effects, *Rev. Environ. Contam. Toxicol.*, 2018, **244**, 5–51.
4 World Health Organization, *Billions of People Still Breathe Unhealthy Air: New WHO Data*, World Health Organization, 2022, vol. 4.
5 C. A. Pope III, R. T. Burnett, M. J. Thun, E. E. Calle, D. Krewski, K. Ito, *et al.*, Lung cancer, cardiopulmonary mortality, and long-term exposure to fine particulate air pollution, *JAMA*, 2002, **287**(9), 1132–1141.
6 D. Loomis, Y. Grosse, B. Lauby-Secretan, F. El Ghissassi, V. Bouvard, L. Benbrahim-Tallaa, *et al.*, The carcinogenicity of outdoor air pollution, *Lancet Oncol.*, 2013, **14**(13), 1262–1263.
7 G. Cipriani, S. Danti, C. Carlesi and G. Borin, Danger in the Air: Air Pollution and Cognitive Dysfunction, *Am. J. Alzheimer's Dis. Other Dementias*, 2018, **33**(6), 333–341.
8 L. Drew, Air pollution and brain damage: what the science says, *Nature*, 2025, **637**(8046), 536–538.
9 G. Oberdorster, Z. Sharp, V. Atudorei, A. Elder, R. Gelein, W. Kreyling, *et al.*, Translocation of inhaled ultrafine particles to the brain, *Inhalation Toxicol.*, 2004, **16**(6–7), 437–445.
10 Y. Qi, S. Wei, T. Xin, C. Huang, Y. Pu, J. Ma, *et al.*, Passage of exogeneous fine particles from the lung into the brain in humans and animals, *Proc. Natl. Acad. Sci. U. S. A.*, 2022, **119**(26), e2117083119.
11 B. A. Maher, I. A. M. Ahmed, V. Karloukovski, D. A. MacLaren, P. G. Foulds, D. Allsop, *et al.*, Magnetite pollution nanoparticles in the human brain, *Proc. Natl. Acad. Sci. U. S. A.*, 2016, **113**(39), 10797–10801.
12 E. Nichols, J. D. Steinmetz, S. E. Vollset, K. Fukutaki, J. Chalek, F. Abd-Allah, *et al.*, Estimation of the global prevalence of dementia in 2019 and forecasted prevalence in 2050: an analysis for the Global Burden of Disease Study 2019, *Lancet Public Health*, 2022, **7**(2), e105–e25.
13 L. Iaccarino, R. La Joie, O. H. Lesman-Segev, E. Lee, L. Hanna, I. E. Allen, *et al.*, Association between ambient air pollution and amyloid positron emission tomography positivity in older adults with cognitive impairment, *JAMA Neurol.*, 2021, **78**(2), 197–207.
14 L. Calderón-Garcidueñas, A. Mora-Tiscareño, M. Styner, G. Gómez-Garza, H. Zhu, R. Torres-Jardón, *et al.*, White matter hyperintensities, systemic inflammation, brain growth, and cognitive functions in children exposed to air pollution, *J. Alzheimer's Dis.*, 2012, **31**(1), 183–191.
15 E. H. Wilker, S. R. Preis, A. S. Beiser, P. A. Wolf, R. Au, I. Kloog, *et al.*, Long-term exposure to fine particulate matter, residential proximity to major roads and measures of brain structure, *Stroke*, 2015, **46**(5), 1161–1166.
16 M. Mortamais, L.-A. Gutierrez, K. de Hoogh, J. Chen, D. Vienneau, I. Carrière, *et al.*, Long-term exposure to ambient air pollution and risk of dementia: Results of the prospective Three-City Study, *Environ. Int.*, 2021, **148**, 106376.
17 M. Lee, J. Schwartz, Y. Wang, F. Dominici and A. Zanobetti, Long-term effect of fine particulate matter on hospitalization with dementia, *Environ. Pollut.*, 2019, **254**(Pt A), 112926.
18 Y. Xie, Z. Liu, T. Wen, X. Huang, J. Liu, G. Tang, *et al.*, Characteristics of chemical composition and seasonal variations of PM2. 5 in Shijiazhuang, China: Impact of primary emissions and secondary formation, *Sci. Total Environ.*, 2019, **677**, 215–229.
19 A. Onoda, T. Kawasaki, K. Tsukiyama, K. Takeda and M. Umezawa, Perivascular Accumulation of β-Sheet-Rich Proteins in Offspring Brain following Maternal Exposure to Carbon Black Nanoparticles, *Front. Cell. Neurosci.*, 2017, **11**, 92.
20 A. Onoda, M. Umezawa, K. Takeda, T. Ihara and M. Sugamata, Effects of maternal exposure to ultrafine carbon black on brain perivascular macrophages and

surrounding astrocytes in offspring mice, *PLoS One*, 2014, **9**(4), e94336.

21 M. Umezawa, A. Onoda, I. Korshunova, A. C. Jensen, I. K. Koponen, K. A. Jensen, *et al.*, Maternal inhalation of carbon black nanoparticles induces neurodevelopmental changes in mouse offspring, *Part. Fibre Toxicol.*, 2018, **15**, 36.

22 T. Suzuki, S. Oshio, M. Iwata, H. Saburi, T. Odagiri, T. Udagawa, *et al.*, In utero exposure to a low concentration of diesel exhaust affects spontaneous locomotor activity and monoaminergic system in male mice, *Part. Fibre Toxicol.*, 2010, **7**, 7.

23 M. Umezawa, H. Tainaka, N. Kawashima, M. Shimizu and K. Takeda, Effect of fetal exposure to titanium dioxide nanoparticle on brain development–brain region information, *J. Toxicol. Sci.*, 2012, **37**(6), 1247–1252.

24 N. Ishihara, T. Okuda, H. Hagino, A. Oguro, Y. Tani, H. Okochi, *et al.*, Involvement of polycyclic aromatic hydrocarbons and endotoxin in macrophage expression of interleukin-33 induced by exposure to particulate matter, *J. Toxicol. Sci.*, 2022, **47**(5), 201–210.

25 Y. Ishihara, T. Takemoto, K. Itoh, A. Ishida and T. Yamazaki, Dual role of superoxide dismutase 2 induced in activated microglia: oxidative stress tolerance and convergence of inflammatory responses, *J. Biol. Chem.*, 2015, **290**(37), 22805–22817.

26 Y. Ishihara, K. Itoh, Y. Mitsuda, T. Shimada, T. Kubota, C. Kato, *et al.*, Involvement of brain oxidation in the cognitive impairment in a triple transgenic mouse model of Alzheimer's disease: noninvasive measurement of the brain redox state by magnetic resonance imaging, *Free Radical Res.*, 2013, **47**(9), 731–739.

27 M. Stefani and C. M. Dobson, Protein aggregation and aggregate toxicity: new insights into protein folding, misfolding diseases and biological evolution, *J. Mol. Med.*, 2003, **81**, 678–699.

28 S. Kaumbekova, M. A. Torkmahalleh, M. Umezawa, Y. Wang and D. Shah, Effect of carbonaceous ultrafine particles on the structure and oligomerization of Aβ42 peptide, *Environ. Pollut.*, 2023, 121273.

29 S. Kaumbekova, M. A. Torkmahalleh and D. Shah, Impact of ultrafine particles and secondary inorganic ions on early onset and progression of amyloid aggregation: Insights from molecular simulations, *Environ. Pollut.*, 2021, **284**, 117147.

30 S. Kaumbekova, M. A. Torkmahalleh, N. Sakaguchi, M. Umezawa and D. Shah, Effect of ambient polycyclic aromatic hydrocarbons and nicotine on the structure of Aβ42 protein, *Front. Environ. Sci. Eng.*, 2023, **17**(2), 15.

31 S. Kaumbekova, M. A. Torkmahalleh and D. Shah, Ambient Benzo[*a*]pyrene's Effect on Kinetic Modulation of Amyloid Beta Peptide Aggregation: A Tentative Association between Ultrafine Particulate Matter and Alzheimer's Disease, *Toxics*, 2022, **10**(12), 786.

32 N. Sakaguchi, S. Kaumbekova, R. Itano, M. A. Torkmahalleh, D. Shah and M. Umezawa, Changes in the secondary structure and assembly of proteins on fluoride ceramic (CeF_3) nanoparticle surfaces, *ACS Appl. Bio Mater.*, 2022, **5**(6), 2843–2850.

33 S. Kaumbekova, N. Sakaguchi, D. Shah and M. Umezawa, Effect of Gold Nanoparticles on the Conformation of Bovine Serum Albumin: Insights from CD Spectroscopic Analysis and Molecular Dynamics Simulations, *ACS Omega*, 2024, **9**(50), 49283–49292.

34 M. Umezawa, R. Itano, N. Sakaguchi and T. Kawasaki, Infrared spectroscopy analysis determining secondary structure change in albumin by cerium oxide nanoparticles, *Front. Toxicol.*, 2023, **5**, 1237819.

35 C. Wallin, S. B. Sholts, N. Österlund, J. Luo, J. Jarvet, P. M. Roos, *et al.*, Alzheimer's disease and cigarette smoke components: effects of nicotine, PAHs, and Cd(II), Cr(III), Pb(II), Pb(IV) ions on amyloid-β peptide aggregation, *Sci. Rep.*, 2017, **7**(1), 14423.

36 S. Nirwal, V. Bharathi and B. K. Patel, Amyloid-like aggregation of bovine serum albumin at physiological temperature induced by cross-seeding effect of HEWL amyloid aggregates, *Biophys. Chem.*, 2021, **278**, 106678.

37 T. I. Chandel, M. Afghani, A. Masroor, I. A. Siddique, S. M. Zakariya, M. Ali, *et al.*, An insight into the inhibition of fibrillation process verses disaggregation of preformed fibrils of bovine serum albumin by isoprenaline hydrochloride, *Int. J. Biol. Macromol.*, 2020, **154**, 1448–1459.

38 M. P. Shevelyova, E. I. Deryusheva, E. L. Nemashkalova, A. V. Machulin and E. A. Litus, Role of Human Serum Albumin in the Prevention and Treatment of Alzheimer's Disease, *Biol. Bull. Rev.*, 2024, **14**(1), 29–42.

39 M. Costa and A. Páez, Emerging insights into the role of albumin with plasma exchange in Alzheimer's disease management, *Transfus. Apher. Sci.*, 2021, **60**(3), 103164.

40 S. A. Tatulian, FTIR analysis of proteins and protein–membrane interactions, *Lipid-Protein Interactions: Methods and Protocols*, 2019, pp. 281–325.

41 M. J. Krysmann, V. Castelletto, A. Kelarakis, I. W. Hamley, R. A. Hule and D. J. Pochan, Self-assembly and hydrogelation of an amyloid peptide fragment, *Biochemistry*, 2008, **47**(16), 4597–4605.

42 M. Tanaka, T. Okuda, K. Itoh, N. Ishihara, A. Oguro, Y. Fujii-Kuriyama, *et al.*, Polycyclic aromatic hydrocarbons in urban particle matter exacerbate movement disorder after ischemic stroke *via* potentiation of neuroinflammation, *Part. Fibre Toxicol.*, 2023, **20**(1), 6.

43 A. Barth and C. Zscherp, What vibrations tell about proteins, *Q. Rev. Biophys.*, 2002, **35**(4), 369–430.

44 X. Huang, G. Tang, J. Zhang, B. Liu, C. Liu, J. Zhang, *et al.*, Characteristics of PM2. 5 pollution in Beijing after the improvement of air quality, *J. Environ. Sci.*, 2021, **100**, 1–10.

45 S. Zhao, H. Tian, L. Luo, H. Liu, B. Wu, S. Liu, *et al.*, Temporal variation characteristics and source apportionment of metal elements in PM2. 5 in urban Beijing during 2018–2019, *Environ. Pollut.*, 2021, **268**, 115856.

46 F. Chiti and C. M. Dobson, Protein misfolding, functional amyloid, and human disease, *Annu. Rev. Biochem.*, 2006, **75**(1), 333–366.

47 V. N. Uversky, α-Synuclein misfolding and neurodegenerative diseases, *Curr. Protein Pept. Sci.*, 2008, **9**(5), 507–540.
48 S. Misra, P. Singh, R. N. Mahata, P. Brandão, S. Roy, A. K. Mahapatra, *et al.*, Supramolecular Antiparallel β-Sheet Formation by Tetrapeptides Based on Amyloid Sequence, *J. Phys. Chem. B*, 2021, **125**(17), 4274–4285.
49 S. K. Mudedla, N. A. Murugan and H. Agren, Free Energy Landscape for Alpha-Helix to Beta-Sheet Interconversion in Small Amyloid Forming Peptide under Nanoconfinement, *J. Phys. Chem. B*, 2018, **122**(42), 9654–9664.
50 M. Karimi, S. Bahrami, S. B. Ravari, P. S. Zangabad, H. Mirshekari, M. Bozorgomid, *et al.*, Albumin nanostructures as advanced drug delivery systems, *Expert Opin. Drug Delivery*, 2016, **13**(11), 1609–1623.
51 B. K. Shanbhag, C. Liu, V. S. Haritos and L. He, Understanding the interplay between self-assembling peptides and solution ions for tunable protein nanoparticle formation, *ACS Nano*, 2018, **12**(7), 6956–6967.
52 S. Kaumbekova, M. Sugita, N. Sakaguchi, Y. Takahashi, A. Sadakane and M. Umezawa, Effect of Acetonitrile on the Conformation of Bovine Serum Albumin, *ACS Omega*, 2024, **9**(48), 47680–47689.
53 P. Khatua, J. C. Jose, N. Sengupta and S. Bandyopadhyay, Conformational features of the Aβ 42 peptide monomer and its interaction with the surrounding solvent, *Phys. Chem. Chem. Phys.*, 2016, **18**(43), 30144–30159.
54 F. Ricchelli, D. Drago, B. Filippi, G. Tognon and P. Zatta, Aluminum-triggered structural modifications and aggregation of β-amyloids, *CMLS Cell. Mol. Life Sci.*, 2005, **62**, 1724–1733.
55 N. Golts, H. Snyder, M. Frasier, C. Theisler, P. Choi and B. Wolozin, Magnesium inhibits spontaneous and iron-induced aggregation of α-synuclein, *J. Biol. Chem.*, 2002, **277**(18), 16116–16123.
56 W. Zhang, H. He, Y. Tian, Q. Gan, J. Zhang, Y. Yuan, *et al.*, Calcium ion-induced formation of β-sheet/-turn structure leading to alteration of osteogenic activity of bone morphogenetic protein-2, *Sci. Rep.*, 2015, **5**(1), 12694.
57 C. Exley, Aluminium and iron, but neither copper nor zinc, are key to the precipitation of β-sheets of Aβ 42 in senile plaque cores in Alzheimer's disease, *J. Alzheimer's Dis.*, 2006, **10**(2–3), 173–177.
58 E. P. DeBenedictis and S. Keten, Mechanical unfolding of alpha-and beta-helical protein motifs, *Soft Matter*, 2019, **15**(6), 1243–1252.
59 L. Liu, Q. Zhou, X. Yang, G. Li, J. Zhang, X. Zhou, *et al.*, Cytotoxicity of the soluble and insoluble fractions of atmospheric fine particulate matter, *J. Environ. Sci.*, 2020, **91**, 105–116.
60 S. Chen, Y. Zhang, H. Chen, W. Zheng, X. Hu, L. Mao, *et al.*, Surface property and *in vitro* toxicity effect of insoluble particles given by protein corona: Implication for PM cytotoxicity assessment, *Eco-Environ. Health*, 2024, **3**(2), 137–144.
61 Y. Zhang, Y. Li, Z. Shi, J. Wu, X. Yang, L. Feng, *et al.*, Metabolic impact induced by total, water soluble and insoluble components of PM2.5 acute exposure in mice, *Chemosphere*, 2018, **207**, 337–346.
62 X. Liu, P. Ge, Z. Lu, M. Cao, W. Chen, Z. Yan, *et al.*, Ecotoxicity induced by total, water soluble and insoluble components of atmospheric fine particulate matter exposure in Caenorhabditis elegans, *Chemosphere*, 2023, **316**, 137672.
63 S. Wei, T. Xu, M. Cao, H. Wang, Y. Song and D. Yin, The Constituent-Dependent Translocation Mechanism for PM2. 5 to Travel through the Olfactory Pathway, *Environ. Health*, 2024, **2**(12), 856–864.
64 M. Mold, C. Linhart, J. Gómez-Ramírez, A. Villegas-Lanau and C. Exley, Aluminum and amyloid-β in familial Alzheimer's disease, *J. Alzheimer's Dis.*, 2020, **73**(4), 1627–1635.
65 M. Sugamata, T. Ihara, H. Takano, S. Oshio and K. Takeda, Maternal diesel exhaust exposure damages newborn murine brains, *J. Health Sci.*, 2006, **52**(1), 82–84.
66 M. Riediker, D. Zink, W. Kreyling, G. Oberdörster, A. Elder, U. Graham, *et al.*, Particle toxicology and health-where are we?, *Part. Fibre Toxicol.*, 2019, **16**, 19.
67 A. Onoda, T. Kawasaki, K. Tsukiyama, K. Takeda and M. Umezawa, Carbon nanoparticles induce endoplasmic reticulum stress around blood vessels with accumulation of misfolded proteins in the developing brain of offspring, *Sci. Rep.*, 2020, **10**, 10028.

